

# AD-P003 148

## ADVANCED COMBUSTOR LINER COOLING CONCEPTS

B. Simon, D. Schubert, U. Basler  
 MTU MOTOREN- UND TURBINEN-UNION MÜNCHEN GMBH  
 P.O.B. 50 06 40  
 8000 München 50, Germany

### SUMMARY

Small gas turbine liner cooling is especially difficult due to the low combustor air flow and relatively large flame tube areas. Therefore, it is desirable to increase the cooling potential of the cooling air by application of combined convective-film cooling. Its advantage must be balanced carefully against the disadvantage of increased weight and production cost.

The large number of variable parameters of a combined cooling configuration requires a computer model which allows the simulation of different cooling approaches. For the verification of this, model tests with various configurations were conducted in a 2D-cooling rig.

Good agreement between measured and calculated liner temperatures could be achieved. Thus, the model is suitable to show under which conditions a marked decrease of wall temperature can be reached compared with the case of straight film cooling under the same conditions.

### SYMBOLS

C/H	-	carbon/hydrogen ratio by weight
L	-	Luminosity factor
P	bar	pressure
T	K	temperature
W	m/s	velocity
x	mm	distance

### Indices

an	annulus
C	cooling air
F	film
FT	flame tube
G	hot gas
Su	not film cooled surface
Sad	adiabatic surface
2D	test model conditions
4	combustor outlet

### 1. INTRODUCTION

The quest for gas turbine engines with higher thrust-to-weight ratio and lower specific fuel consumption entails increasing turbine entry temperatures and pressure ratios. In accordance with Ref. 1 the pressure ratios in the 1000 kW engine bracket are expected to grow from a present 12 to 20, and the turbine entry temperatures from 1400 K to 1600 K and over. For combustion chamber applications, this means that the temperature of the hot gases, as well as that of the compressor air used for cooling purposes, is bound to grow. Accordingly, wall temperatures will rise unless inhibited by a higher allotment of cooling air or by an improved cooling method doing a more effective job. The relationship will become apparent from Fig. 1, where the effects of pressure ratio and turbine entry temperature have been combined in accordance with Ref. 2 into a parameter plotted on the abscissa, while the ordinate represents the cooling air requirement for the respective flame tube surface area. The shape of the curve qualitatively reflects the relationship between these two quantities for straight film cooling. Below the shaded area is the region in which the flame tube walls are undercooled, and above it they are overheated.

The engine points on the graph were determined on the assumption that 60 % of the combustion chamber air is allotted to wall cooling and that 1270 K is the maximum allowable wall temperature. At these conditions the combustion chambers of large engines like the CF6-50 and PWA 2037 are just about undercooled, so that the cooling air flow could safely be reduced or the cooling method be less effective.

Not so with small engines, where at a pressure ratio of 13 and a turbine entry temperature of 1550 K, a fully 60 % share of the cooling air supply is not enough to cool the flame tube. The patently different cooling requirements of small versus large engines is explained by differences in construction. With small engines, coming with a centrifugal-flow final compressor stage as they generally do, the preference is for reverse-flow annular combustion chambers, which mate up well with the centrifugal-flow compressor. While this gives an advantageously short, compact construction to the engine, for which see Fig. 2, it makes the surface of the combustion chamber unproportionately large, because of its location above the turbine. Add to this the deflector elbow, which deviates the combustion gases to the turbine through an angle of 180° and equally requires cooling. All of which puts much more emphasis on combustor cooling problems than is standard in big-engine work.

For the small engines, therefore, more effective cooling methods to give more cooling power for the same if not reduced cooling air input is called for. This greater cooling effectiveness can be achieved by preceding film cooling with convective outer surface cooling for improved utilisation of the cooling capacity of the air. Fig. 3 illustrates various approaches to convective outer surface cooling, which may be of the impingement or the convection duct type.

For both cooling methods, there exists a large number of parameters with which to affect cooling. In impingement cooling this would be, mainly, the pattern and size of impingement holes, the depth of duct, and selective allocation of the impingement and film cooling shares of the total pressure loss of the cooling figuration. With the convection duct, the depth of duct and the type and effective roughness of fitted items, such as spoilers, fins, pimples and pins all play a part as well.

The cooling effect can in either case be controlled additionally by the manner in which the flow is routed in convection and film cooling. As shown in Fig. 3 the flow can be parallel, counterflow or parallel and counterflow combined.

As it will already have become apparent from the schematic arrangements of Fig. 3, design feasibility is an important aspect to consider in the selection of a cooling method. While this aspect is set aside in the present paper, it is nevertheless admitted that added complexity of design will as an immediate drawback entail cost and weight penalties. Before contemplating the embodiment of cooling methods in hardware designs, therefore, one should have proper proof that the total effectiveness of the combined convection and film cooling methods will be clearly superior to that of straight film cooling; otherwise, the effort would not be warranted.

Investigations into cooling configurations in a realistic combustion chamber environment are rather impracticable, owing to the high pressures and temperatures involved. More moderate temperatures and ambient pressures substantially facilitate testing, but are suspected to compromise results. For truly representative evidence, not only the geometric similarity but also the pressure loss across the cooling configuration, the Reynold's numbers inside and outside of the hot gas wall and finally the mass flow and temperature ratios of hot gas to cooling film entry air would have to be kept constant. This being an onerous job, an alternative approach is here attempted, where the results obtained under test rig conditions are reproduced by means of a newly evolved computational procedure. The rig tests, accordingly, merely serve to verify the general validity of the computational procedure, and no attempt is made to assess the cooling method on the strength of rig test evidence. Actual comparison of the relative merits of the various cooling methods is then made by computation at small gas turbine level.

## 2. TESTS

### 2.1 Test Setup and Conditions

Fig. 4 is a schematic arrangement of the rig setup used in testing cooling effectiveness. The respective test specimen separates the cooling air duct from the hot air duct in the test section.

Having passed through an air heater, the heated air reaches the test section through an insulated rectangular-section duct. A spoiler grid produces the intended degree of turbulence in the hot air duct. In plane 1 on the sketch a probe can be traversed in three directions.

The cooling air enters the secondary air duct from above. The respective setting for the cooling air to hot air duct pressure ratio allows cooling air to flow through the test specimen and into the hot air duct. The air bypassing the test specimen issues from the rig through a pipe line.

In the experiments designed to test the effectiveness of the cooling film the secondary air duct was sealed off in the test specimen area by an insulation layer.

The tests were run at the following standard conditions:

$T_G$	=	873 K
$T_C/T_G$	=	0.4
$W_G$	=	50 m/s
$T$	=	3 %
$W_{an}$	=	18 m/s (at tests without insulation)

### 2.2 Description of Test Specimens

Three different cooling methods were investigated:

- straight film cooling
- combined impingement / film cooling
- convection duct cooling

For each cooling method, two specimens were available (cf. Fig. 5). The film cooling specimens F1 and F2 are identical in construction except for the free flow area. The test specimen F1, which was designed to represent a configuration for a large-size combustion chamber, has 3.8 times the flow area of test specimen F2. The unconventional form of the test specimens comes as a result of two considerations: One, the lip was to be as short as possible, for which the additional length of passage that was needed to

blend the discrete incoming jets into a film was obtained by deflection. Two, a configuration of this type is suitable for producing combined impingement/film cooling, which operates on the counterflow principle. As it will become apparent from Fig. 5 the test specimens PF1 and PF2 were produced simply by tack-welding perforated plates to the film cooling specimens F1 and F2. The perforation of the plates is indicated in Tab. 1.

The convection duct specimens KF1 and KF2 are made of two cover plates separated by a corrugated metal sheet forming cooling passages. For improved heat transfer, the metal sheets either form off-set fins as with test specimen KF1, or are slotted as with test specimen KF2.

### 2.3 Test Results

First, the flow characteristics of all test specimens were charted. Plotted in Fig. 6 is the reduced mass flow versus pressure loss. As it will readily become apparent the test specimens F1 and PF1 exhibit a considerably larger flow than F2 and PF2. The cover plates of the combined impingement/film cooling configuration were designed to have about 25 % of the pressure loss caused by the impingement holes. Another 35 % of the pressure loss was caused by the air dedicated to film cooling. The duct flow causes the greatest pressure loss. The effective area of the film cooling holes varied with the presence or absence of the cover plate, the  $C_p$  value improving when a cover plate was tacked in place. Flow differences of similar magnitudes were noted also for test specimens KF1 and KF2. The test specimens with the large flows simulated combustion chamber environments in large engines, while those with the small flows were typical of conditions in the reverse-flow annular combustion chambers used in small gas turbine engines.

Fig. 7 shows the cooling film effectiveness of cooling film configurations F1 and F2 versus the Odger Winter parameter, which in accordance with Ref. 3 represents a correlation quantity permitting effectiveness to be evaluated at randomly selected conditions. The cooling film effectiveness was evaluated in accordance with the following equation:

$$\eta_F = \frac{T_{Su} - T_{Sad}}{T_{Su} - T_C}$$

where  $T_{Su}$  is the temperature of the insulated specimen wall in the absence of film cooling, and  $T_{Sad}$  is the temperature of the insulated wall with film cooling applied.

Obviously the results obtained with cooling film F1 can readily be correlated, while for cooling film F2, the pressure loss makes itself clearly felt. It is suspected that the air flow diverted for cooling film F2 does not fully fill the film gap and that the thickness of film varies with the pressure loss. This property remaining intact at elevated pressures and temperatures, however, the results will also in that form be acceptable for subsequent extrapolation to engine applications.

The Nusselt numbers in the duct of test specimens KF1 and KF2 were first determined separately in a special rig, with the results shown in Fig. 8. They are needed for computational verification of the evidence obtained on the cooling test rig. The Nusselt number of test specimen KF1 is greater than that of KF2 at the same Reynolds number over a wide range.

Fig. 9 shows typical readings taken on the test specimens PF1 and KF1. In both cases, thermal conduction effects were apparent. On test specimen KF1 the cooling air forms a film at the end of the duct and operates in the manner of film cooling. Combination of film with convection cooling was deliberately omitted, because it was intended to first isolate the detail effects. It is envisioned to couple the two effects together by computation at a later date.

Comparison of the two cooling methods was not attempted. Conditions underlying the respective measurements were too different for true comparison - the flow being much higher for KF1 but in the absence of the film cooling enjoyed by PF1. Yet the measurements were not intended to support an assessment of the cooling methods. The intention rather was to obtain readings suitable for comparison with computed values. The computational procedure used for the purpose is described below.

### 3. COMPUTATIONAL PROCEDURE

The computational procedure bases on a one-dimensional heat flow model as it is illustrated in Fig. 10 by way of a control volume of the cooling configuration. On the hot gas side, heat transfer is by radiation and convection, after which the heat is conducted through the hot gas wall, with a thermally insulating layer being optionally considered. In the convection duct the heat picked up by the air axially must be allowed for, apart from the heat transfer between the gas and the wall. The heat transfer to the secondary duct again is by conduction, convection and radiation.

The metal plate used in the construction of combustion chambers being rather thin, axial thermal conduction was ignored.

#### 3.1 Heat Transfer on the Hot Gas Side

Heat transfer on the hot gas side is by radiation and convection. To determine the convection term, resort was made to the cooling film effectiveness measurements.

Turbulence in the combustion chamber flow can be considered in accordance with Ref. 4 by the following statement:

$$\frac{\eta_{FT}}{\eta_{2D}} = \frac{1 + \frac{T_{2D} \times s}{100 M}}{1 + \frac{T_{FT} \times s}{100 M}}$$

where M is the mass flow density ratio of cooling air to hot gas at the film entry, and s is the depth of slot. On the 2-D-rig, a spoiler grid was used to maintain a turbulence intensity of a constant 3 %. LDA measurements taken at the exit of a Larzac combustion chamber (Ref. 5) indicate a turbulence intensity of 15 %. In accordance with Ref. 6, however, the turbulence is assumed to be less in a reverse-flow annular combustion chamber, owing to the lower reference speed. The value assumed for the reverse-flow annular combustion chamber, therefore, was 9 %.

In hot gas radiation, a great amount of uncertainty exists regarding the luminosity factor, which allows for augmentation of gas radiation by smoke particles. In accordance with Ref. 3 the luminosity factor is formed as a function of fuel composition in accordance with the following equation:

$$L = 0.0691 (C/H - 1.82)^{2.71}$$

This equation was used in the computation of hot gas radiation. The formulation for the exchange of radiation between the gas and the wall was made in accordance with Ref. 7.

### 3.2 Heat Transfer in the Convection Duct

Heat transfer in the convection duct was determined for impingement cooling using Nusselt numbers stated in Ref. 8. They base on measurements taken over a wide range of jet Reynolds numbers. This effective range also covers the constellation encountered with the combustion chamber.

If the convection duct would be finned, use could either be made of measured Nusselt numbers, or the Nusselt numbers could be computed via the fin efficiency. Various fin geometries, such as rectangular or triangular, could be selected.

Exchange of radiation in the convection duct is limited to that between the walls. The cooling air can be routed in the convection duct in either parallel or counterflow.

### 3.3 Heat Transfer to the Combustion Chamber Annulus

On the outside of the flame tube wall, heat transfer occurs by convection to the combustion chamber secondary air and by radiation to the combustion chamber casing.

Use was made of a duct relation to determine the heat transfer coefficient.

## 4. COMPARISON BETWEEN MEASUREMENT AND COMPUTATION AT MODEL TEST RIG CONDITIONS

Fig. 11 compares the wall temperatures in the presence of cooling films F1 and F2. In both cases the test rig conditions described in Chapter 2 were maintained. Unlike in earlier presentations of cooling film effectiveness the outer wall of the test specimen was not insulated; the flow velocity in the secondary duct was 18 m/s.

Agreement of the test points with the computed curves is excellent over the entire flow path tested.

Fig. 12 is a comparison between measurement and computation for the combined impingement/film cooling and the convective duct cooling methods.

In impingement/film cooling the deviation of the computed axial temperature variation over the entire test section does not exceed 2.5 %. It is solely the last test point, lying as it does in the impingement cooled section of the test specimen, which exhibits a greater amount of deviation. This is attributable to axial heat conduction effects ignored in the computation model.

In the case of convection cooling the measurement was made in the absence of film cooling. The outside of the test specimen was insulated for maximum freedom from interference with the measurements. In this case, again, the only major deviation of the computed from the measured results was at the edge of the test specimen, which is again attributable to axial conduction effects. On balance the computational model makes sufficiently accurate predictions of the temperature profile of the test specimen wall.

## 5. ASSESSMENT OF THE VARIOUS COOLING METHODS

### 5.1 Comparison at Test Rig Conditions

From the cooling aspect, comparison of the three cooling methods one with the other is of special interest. This comparison is shown in Fig. 13, which illustrates the cooling configurations P2, PF2 and KP2, with the amount of cooling air being the same for all three. The test specimen KP2 had film cooling applied additionally, when it was assumed that film cooling was caused by a preceding configuration identical to KP2. In contrast with the previously shown configurations the cooling air flow is substantially

less and approximately corresponds to conditions encountered in the reverse-flow annular combustion chamber of a small gas turbine.

At these conditions, impingement film cooling makes for no lower wall temperatures than straight film cooling, for the reason that the film cooling effect, which is compromised by the heat imparted to the cooling air, cannot be overcompensated by the improved external heat transfer. Conceivably, optimisation of the local pattern and size of impingement holes and the depth of duct might lead to somewhat lower the temperature and alleviate especially the axial temperature gradient; in the final analysis, however, impingement cooling will - at 2D rig conditions simulating a small engine combustion chamber - afford the advantage of a more homogeneous temperature distribution.

The highest wall temperatures were found for the convective duct/film cooling which results from low heat transfer in the convection duct in combination with poor effectiveness of the cooling film under test model conditions.

## 5.2 Comparison at Combustion Chamber Conditions

For definition of combustion chamber flow conditions, the type of combustion chamber and the size of engine should be specified, considering that the amount of cooling air available varies importantly with these boundary conditions. The present paper takes a look at typical conditions in the combustion chamber area of a small engine. Fig. 14 shows the combustion chamber of this engine. The thermodynamic cycle conditions of this combustion chamber are:

$$\begin{aligned} P_{an} &= 13 \text{ bar} \\ T_C &= 667 \text{ K} \\ M_4 &= 3.2 \text{ kg/s} \\ T_4 &= 1550 \text{ K} \end{aligned}$$

Further important data entering into the wall temperature calculation are the local flow and hot gas temperature conditions. These obviously vary with the axial position along the combustion chamber. With reverse-flow combustion chambers, changes are especially drastic. Flow conditions may be prevailing on the outer liner, e.g., at which the secondary flow moves in a direction counter that of the hot gas or film flow. For straight film cooling, this may have notable impact on wall temperatures.

For the wall temperature calculation, the following significant quantities were selected:

$$\begin{aligned} W_G &= 10 \text{ m/s} \\ Ma_{an} &= 0.038 \quad W_{an} = 20 \text{ m/s} \\ T &= 9 \text{ s} \end{aligned}$$

For these conditions the computer model was used to determine the wall temperature profile for the three different cooling methods, when a 3 % pressure loss was maintained in all cases and the air flow through the configuration was a constant 4 %. In the case of configuration KF2 these conditions can be established by using suitable perforations at the inlet.

The result is shown in Fig. 15.

Straight film cooling makes for the highest wall temperatures and the steepest wall temperature gradients when film and secondary air flows run in the same direction. This cooling method would appear much more promising - in regard to both peak temperature and temperature distribution - if the secondary flow is made to run counter the film, as it is the case on the outer liner of the flame tube.

Compared with this constellation the combined impingement/film cooling method affords no essential advantage, although admittedly the configuration used was, again, no optimised solution, but rather the standard configuration of Tab. 1.

The combined convection duct/film cooling method is the most effective of the lot. Compared with impingement cooling the maximum wall temperature was lowered by 100 K, and compared with film cooling in counterflow, by 150 K. The effectiveness can still be improved when use is made of the counterflow principle. This very much levels the temperature distribution and the temperature peak is again reduced.

The question surfaced whether or not the superiority of the convection/film cooling method might be due to the failure to optimize the impingement/film configuration. It was therefore attempted to improve the cooling effectiveness by varying the depth of duct, the diameters, the number of impingement holes or the stagger of the rows of holes (see Tab. 1). The results are shown in Fig. 16. While starting from the basic configuration the above changes indeed improves the effectiveness, this amounted to relatively modest reduction of some 30 K in the maximum temperature.

Conceivably the temperature could be made more uniform if impingement holes of various diameters axially were used. Calculation was prevented, however, for the lack of Nusselt relations for this case.

## 5.3 Potential Cooling Air Savings

From the practical combustion chamber development aspect the objective is not to use improved cooling methods to lower wall temperatures below the level achieved with present methods. Rather, it is attempted to achieve the same wall temperatures despite reductions

in the amount of cooling air expended. Fig. 17, therefore, shows how much cooling air can be economised if combined convection/film cooling is used in comparison to straight film cooling.

The comparison was made for the standard combustion chamber conditions previously defined. The cooling air flow at film cooling was 4 % of the entire combustion chamber air. At these conditions the combined convection/film cooling method required only nearly one-half of the air being used in straight film cooling at parallel flow conditions.

## 6. CONCLUSIONS

The use of combined cooling methods has its merits only where it clearly raises the cooling effectiveness over straight film cooling. This effectiveness, therefore, first needs analysing. Test rig measurements will provide no conclusive evidence, because it is limited to a few configurations. Also, the rig testing effort becomes prohibitive when it is attempted to test at actual combustion chamber conditions. Measurements taken on the model test rig nevertheless show that as an immediate gain, no convincing advantages over straight film cooling can be achieved using combined cooling methods at reduced conditions.

The test results, therefore, were essentially used to verify a computer procedure developed to test the effectiveness of diverse cooling configurations and subsequently extrapolate them to the conditions prevailing in a small reverse-flow annular combustion chamber.

It was then seen that the convection duct/film cooling method gave the best effectiveness by far.

A very important consideration in the assessment of the impingement/film cooling method is what the local combustion chamber flow conditions are. If there exists a strong flame tube outside flow in a direction counter the flame tube flow, as it is often the case with reverse-flow annular combustion chambers, this combined method provides little if any advantage over straight film cooling. But if the outside flow is moderate, as in the rear region of the inner liner, considerable advantages may result over the straight film cooling method, because impingement cooling will provide the convective outer flow that otherwise would be missing.

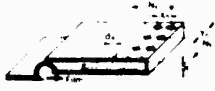
The use of combined convection/film cooling configurations is made difficult by the high stresses set up between the two duct walls. The design effort required to take care of these is considerable and involves cost and weight penalties. Ultimately, then, use will be made of the cooling method that gives adequate cooling for the least investment. Judgement in the matter will rest on the existence of safe methods of forecasting the wall temperatures.

## Acknowledgment

Part of the work reported was financed by the German Ministry of Defence. This support is gratefully acknowledged.

## 8. REFERENCES

- 1 Demetri, E.P. et al., "Study of Research and Development Requirements of Small Gas Turbine Combustors", NASA CR-159796 (1980)
- 2 Henderson, R.E., "Turbopropulsion Combustion Technology Assessment", AFAPL-TR-2115 (1980)
- 3 Kretschmer, D., Odgers, J., "A Simple Method for the Prediction of Wall Temperatures in Gas Turbines", ASME No. 78-GT 90 (1978)
- 4 Marek, C.J., Tacina, R.R., "Effect of Free Stream Turbulence on Film Cooling", NASA TN D 7958 (1975)
- 5 Schäfer, H.G., Koch, B., Horny, G., Masure, B., "Laseranemometrisch Messungen der mittleren Geschwindigkeit und des Turbulenzgrades in der Austrittsebene einer Brennkammer des Typs Larzac", Techn. Bericht RT 513/77 (1977)
- 6 Norgren, C.T., Riddlbaugh, S.M., "Small Gas Turbine Combustor Study - Combustor Liner Evaluation", AIAA No. 83-0337 (1983)
- 7 Lefevbre, A.H., Herberts, M.V., "Heat Transfer Processes in Gas Turbine Combustion Chambers", Proceedings of the Institution of Mechanical Engineers, Vol. 174,12, (1960)
- 8 Florschuetz, L.W., Truman, C.R., Metzger, D.E., "Streamwise Flow and Heat Transfer Distributions for Jet Array Impingement with Crossflow", ASME No. 81-GT-77, (1981)



Reverse flow combustor  
Conditions for PF2  
P = 3% M<sub>2</sub> = 4%

PF1	Test model configuration	d <sub>1c</sub>	d <sub>2c</sub>	N <sub>2</sub>	d <sub>3c</sub>	N <sub>2</sub>	
		mm	mm		mm		
	1 Basic configuration	18	194	5	5.55	15	
	2 Reduction of channel height	0.85	1	4	7.35	179	
PF2 (see Fig. 16)	3 Decrease number of holes in x- and y direction	1.13	2	3		134	
	4 Decrease number of holes in x-direction Increase number of holes in y direction	0.85			9.46	5.68	274

Tab. 1: Hole Configurations of the Impingement Plates

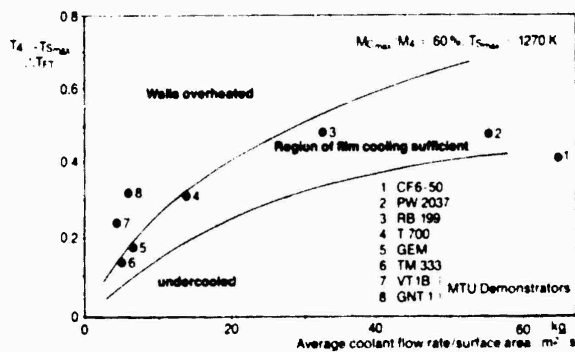


Fig. 1: Coolant Demand for Film Cooling

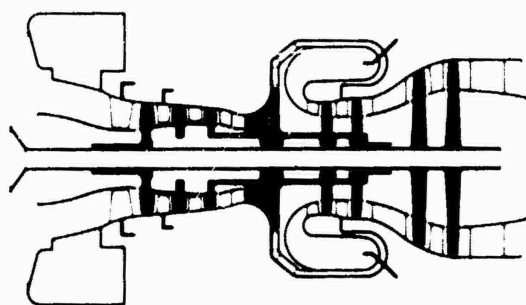


Fig. 2: Scheme of a Small Gas Turbine with Reverse Flow Combustor

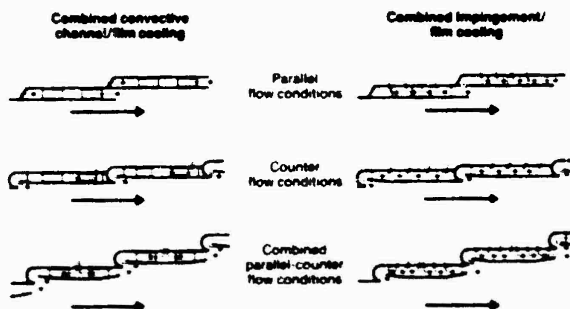


Fig. 3: Combined Cooling Methods

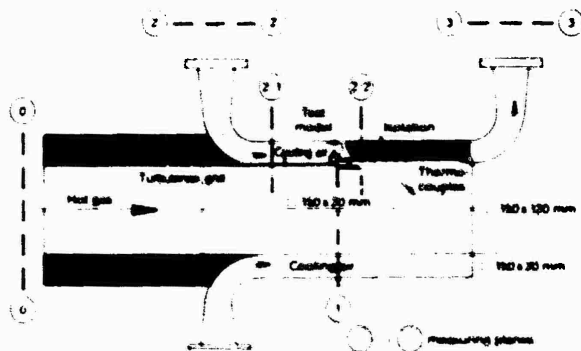


Fig. 4: Film Cooling Test Section

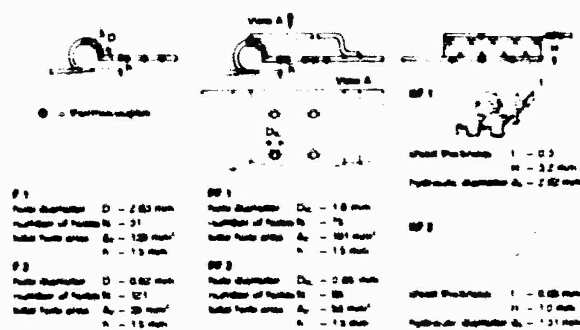


Fig. 5: Film Cooling Test Specimens

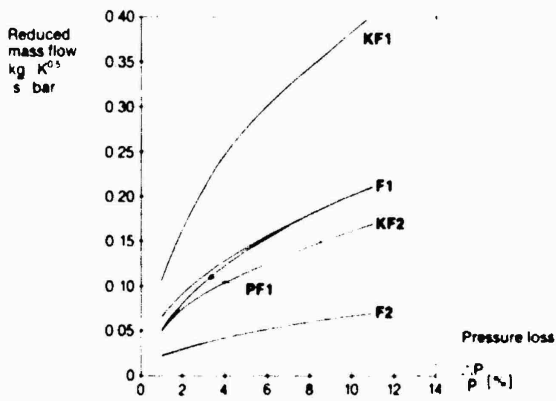


Fig. 6: Mass Flow Characteristics for Test Specimens F1, F2, PF1, KP1, KF2

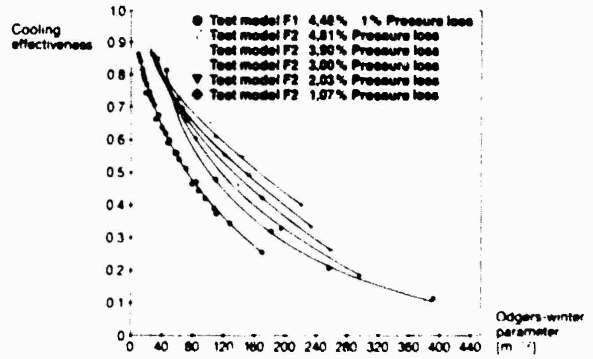


Fig. 7: Film Cooling Effectiveness of Configuration F1, F2

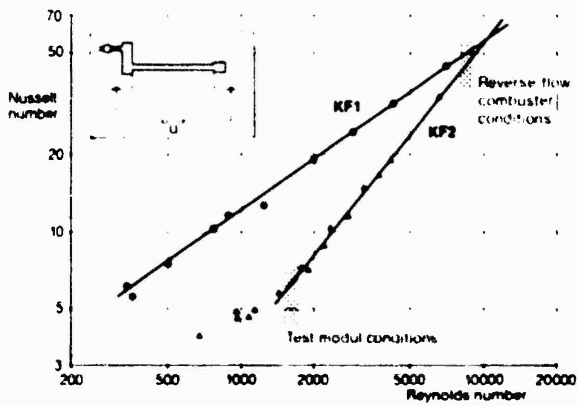


Fig. 8: Nusselt Number for KF1 and KF2

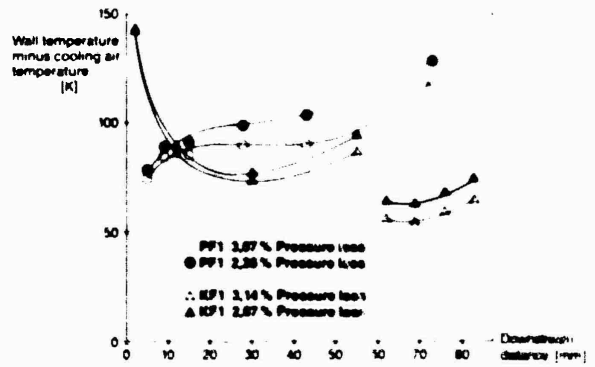


Fig. 9: Wall Temperature Distribution for PF1 and KF1

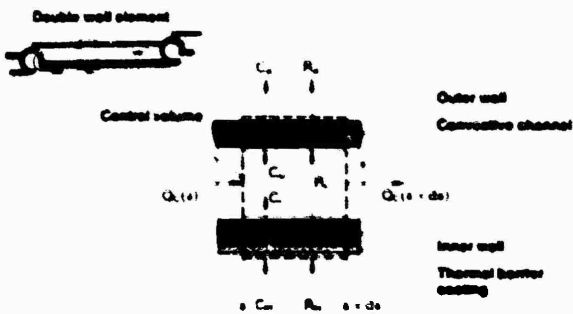


Fig. 10: Analytical Model

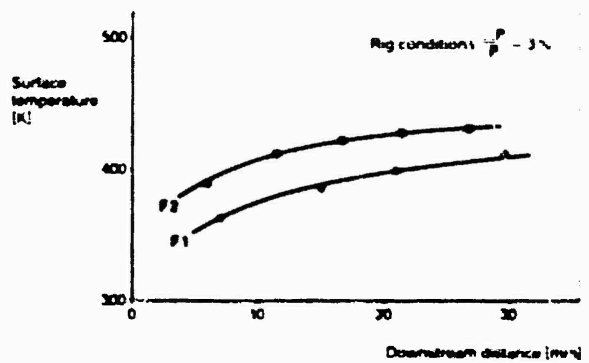


Fig. 11: Comparison of Measured and Calculated Surface Temperatures for Pure Film Cooling



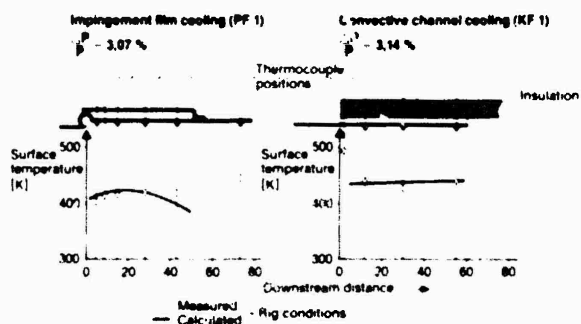


Fig. 12: Comparison of Measured and Calculated Surface Temperatures

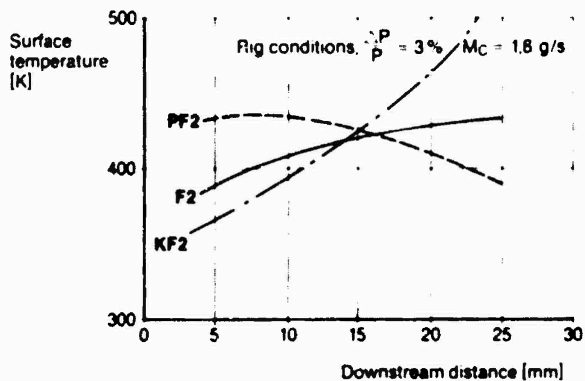


Fig. 13: Comparison of Different Cooling Methods under Rig Conditions

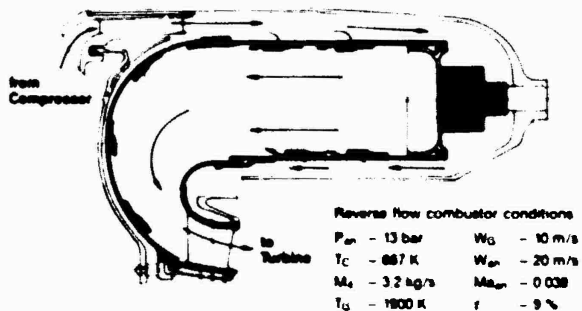


Fig. 14: Reverse Flow Combustor

Reverse flow combustor conditions  
 $P_{in} = 13 \text{ bar}$      $W_D = 10 \text{ m/s}$   
 $T_C = 887 \text{ K}$      $W_{in} = 20 \text{ m/s}$   
 $M_c = 3.2 \text{ kg/s}$      $M_{in} = 0.038$   
 $T_G = 1800 \text{ K}$      $r = 9\%$

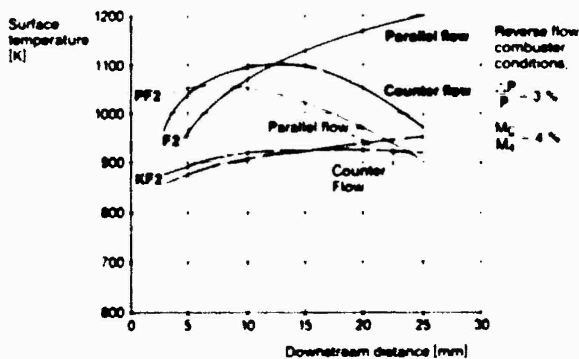


Fig. 15: Surface Temperatures for Different Cooling Methods

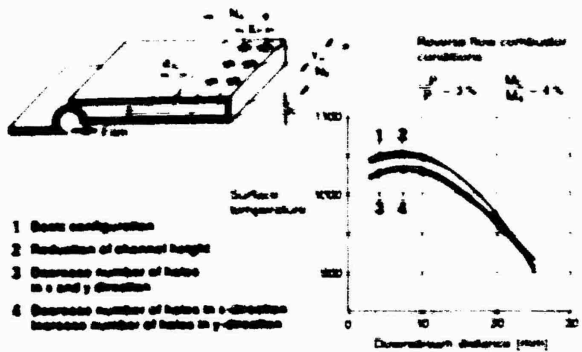


Fig. 16: Variation of Multi Hole Impingement Configuration

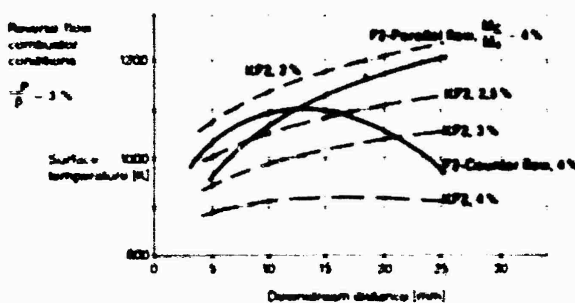


Fig. 17: Reduction of Cooling Air Demand by Combined Convective-Film Cooling

## DISCUSSION

**K.Collin**

- (1) What is the length of the film cooling specimens?
- (2) Do you optimize this length for pressure drop?
- (3) Have you a feeling about the cost penalties of the three film cooling schemes?

**Author's Reply**

- (1) The length of the film cooling specimens was about 70 mm.
- (2) In the case of the combined convective channel-film cooling configuration only a very low dependence of the pressure drop on the length of the specimen was observed. The greatest contribution to pressure loss resulted from a row of metering holes in the front of the configuration.
- (3) Estimation of cost penalties of the combined methods is only possible if the difference of the cooling effectiveness of all three methods is well known. To investigate the latter was the task of this paper. Cost problems should be considered in connection with a practical application.

**D.Snape, UK**

Have you made any attempts to understand the fundamental processes of impingement type cooling, e.g. by maintaining the effects of hole diameter pitch ratio? If so, do you have any indications of how impingement effectiveness can be optimized?

**Author's Reply**

We tested some variations in hole diameters, pitch ratio and channel height. These investigations are given in the paper but they are very limited. Optimal configurations should include the variation of the hole diameter in the axial direction. Those configurations could not be calculated because of the lack of suitable heat transfer numbers.

**P.Ramette, Fr**

Avez vous fait une comparaison des contraintes thermiques dans les matériaux pour les trois types de refroidissement que vous avez étudiés?

**Author's Reply**

Not yet. We first wanted to know which cooling type gives the best effectiveness. This will be studied later.